Technische Universität Chemnitz

Sonderforschungsbereich 393

Numerische Simulation auf massiv parallelen Rechnern

Karsten Eppler Helmut Harbrecht

Numerical Studies of Shape Optimization Problems in Elasticity using wavelet-based BEM

Preprint SFB393/01-29

Preprint-Reihe des Chemnitzer SFB 393

SFB393/01-29 **November 2001**

Contents

Author's addresses:

Karsten Eppler
Helmut Harbrecht
TU Chemnitz
Fakultät für Mathematik
D-09107 Chemnitz

http://www.tu-chemnitz.de/sfb393/

Introduction - a shape problem in planar elasticity

We consider a cylindric circular bar which is homogeneous and isotropic with a planar, simply connected cross section $\Omega \in \mathbb{R}^2$. We follow Banichuk and Karihaloo [2] but normalize the shear modulus $G = 1$ and the elastic modulus $E = 1$. We want to solve the problem of maximizing the bending stiffness of the bar subject to given inequality constraints on the torsional rigidity and the volume. In addition, we study related problems. We minimize the volume, where bounds for the torsional and bending stiffness are given. Further, we maximize the torsional rigidity subject to volume and bending constraints, respectively.

After the formulation of the three classes of problems we introduce a simple approach for performing the shape calculus. The idea is based on the assumption that the cross sections Ω under consideration are uniformly starshaped with respect to an open ball $U_\delta(\overline{\mathbf{x}}) \subset \Omega$. Without loss of generality we set $\overline{\mathbf{x}} = \mathbf{0}$ in the sequel. For a first order calculus we assume regular domains $\Omega \in C^2$. Clearly, Ω can be identified with a boundary describing function for $\Gamma = \partial\Omega$, i.e., in polar coordinates we have

$$\Gamma := \Big\{ \gamma(\phi) = r(\phi) \left[\begin{smallmatrix} \cos\phi \\ \sin\phi \end{smallmatrix} \right] : \phi \in [0, 2\pi] \Big\},$$

where $r \in C^2_{\rm per}[0, 2\pi]$ is a positive function with

$$C^2_{\rm per}[0, 2\pi] = \{ r \in C^2[0, 2\pi] : r^{(i)}(0) = r^{(i)}(2\pi),\ i = 0, 1, 2 \}. \tag{0.1}$$

As a standard variation for perturbed domains Ω_ε and boundaries Γ_ε, respectively, we introduce a function $dr \in C^2_{\rm per}[0, 2\pi]$

$$r_\varepsilon(\phi) = r(\phi) + \varepsilon dr(\phi),$$

where $\gamma_\varepsilon(\phi) = r_\varepsilon(\phi)\mathbf{e}_r(\phi)$ is always a Jordan curve. Herein, $\mathbf{e}_r(\phi) = \left[\begin{smallmatrix} \cos\phi \\ \sin\phi \end{smallmatrix} \right]$ denotes the unit vector in the outer radial direction. Note that the normal direction is given by

$$\mathbf{n}(\phi) = \frac{1}{\sqrt{r^2(\phi) + r'^2(\phi)}} \begin{bmatrix} r(\phi)\cos\phi + r'(\phi)\sin\phi \\ r(\phi)\sin\phi - r'(\phi)\cos\phi \end{bmatrix}.$$

The main advantage of this simple approach is a complete embedding of the shape problem into a Banach space setting. That is, at least for a first order calculus, *both*, the shapes and its increments, can be viewed as elements of $C^2_{\rm per}[0, 2\pi]$. For the sake of brevity, we do not list completely the approaches for the description of domain or boundary variations which are available also for more general shapes. Moreover, we do not discuss the applications and the further methods for the numerical solution. To that aim, we only refer to the monographs Pironneau [25], Haslinger and Neitaanmaeki [24] and Sokolowski and Zolesio [29] and the references therein.

In order to solve the given infinite dimensional optimization problems approximately, we transform them to finite dimensional auxiliary problems. Then, we apply standard methods for the optimization of these finite dimensional problems. Because the basics of such optimization algorithms are well known, we mainly focus on the related theoretical and implementational aspects. Consequently, we give only a few references and not a complete overview about the existing literature.

The torsional rigidity with respect to a given domain is defined by a partial differential equation for the stress function. We emphasize that this stress function has to be computed on different domains a lot of times during the optimization algorithm. In particular, this has to be done not only once in each iteration but also in the line search. Hence, it is clear that we spent effort in order to make its computation cheap. As we show in this paper, the knowledge of its normal derivative suffices to evaluate the data appearing from the torsional rigidity. Invoking a Newton potential, the normal derivative can be represented by a Dirichlet-to-Neumann map based on boundary integral operators, namely the single layer operator and the double layer operator. The application of boundary elements for the discretization requires only a partition of the boundary. Therefore, we do not need a triangulation of the domain like for finite elements.

In general, boundary element methods suffer from a major disadvantage. The corresponding system matrices are densely populated. Therefore, the complexity for solving such equations grows at least quadratic with the number of equations. This fact restricts the maximal size of the linear equations seriously. Modern methods for the fast solution of BEM reduce the complexity to a suboptimal rate or even an optimal rate, that is a linear rate. Prominent examples for such methods are the *fast multipole method* by Greengard and Rokhlin [18] and the *panel clustering* by Hackbusch and Novack [20]. Observed first by Beylkin, Coifman and Rokhlin [4], the *wavelet Galerkin scheme* offers another tool for the fast solution of integral equations. In fact, a Galerkin discretization based on wavelet bases results in numerically sparse matrices, i.e., many matrix entries are negligible and can be treated as zero. Discarding these nonrelevant matrix entries is called matrix compression. In accordance with Dahmen et al. [7, 10, 9, 28], this can be performed without compromising the accuracy of the underlying Galerkin scheme. As shown by Dahmen, Harbrecht and Schneider in [7, 23, 28], the wavelet Gelerkin scheme has an optimal over-all complexity.

The paper is organized as follows. Section 1 is dedicated to the modeling, shape calculus and the necessary conditions of the optimization problems. In section 2 we transform the infinite dimensional optimization problems to finite dimensional

ones. In order to optimize them, we apply descent methods of first order. The fast solution of the state equation is considered in section 3. In section 4 we present various numerical experiments. They confirm the theory as well as the power of our algorithms.

1. Modeling, stationary solutions and shape calculus

1.1. **The optimization problems.** First, we introduce the mathematical formulation of the quantities. Moreover, we give the related expressions in polar coordinates, if this is possible explicitly.

The bending rigidity with respect to a fixed barycentre in the origin, see remark 1.1 below, is given by

$$B(\Omega) = \int_\Omega y^2 d\mathbf{x} = \frac{1}{4}\int_0^{2\pi} \sin^2\phi r^4(\phi) d\phi \tag{1.1}$$

where $\mathbf{x} = [x, y]^T$. The torsional rigidity is calculated by

$$T(\Omega) = 2\int_\Omega u(\mathbf{x}) d\mathbf{x} = \int_0^{2\pi}\int_0^{r(\phi)} u(\rho,\phi)\,\rho d\rho d\phi, \tag{1.2}$$

where the stress function $u = u(\Omega)$ satisfies

$$\begin{aligned} \Delta u &= -2 \quad \text{in } \Omega, \\ u &= 0 \quad \text{on } \Gamma. \end{aligned} \tag{1.3}$$

For the volume of the domain and its barycentre we find

$$\begin{aligned} V(\Omega) &= \int_\Omega d\mathbf{x} = \frac{1}{2}\int_0^{2\pi} r^2(\phi) d\phi, \\ \mathbf{x}_b(\Omega) &= \left[\begin{smallmatrix} x_b(\Omega) \\ y_b(\Omega) \end{smallmatrix}\right] = \frac{1}{V(\Omega)}\int_\Omega \mathbf{x} d\mathbf{x} = \frac{1}{3V(\Omega)}\int_0^{2\pi} \left[\begin{smallmatrix} \cos\phi \\ \sin\phi \end{smallmatrix}\right] r^3(\phi) d\phi. \end{aligned}$$

Remark 1.1. *The constraint $y_b = 0$ is urgently needed for making correct the definition of the bending functional via* (1.1)*, whereas $x_b = 0$ is introduced only for fixing the problem with respect to a shift in x-direction. Moreover, the use of the modified barycentre coordinates*

$$\widehat{\mathbf{x}}_b(\Omega) = \left[\begin{smallmatrix} \widehat{x}_b(\Omega) \\ \widehat{y}_b(\Omega) \end{smallmatrix}\right] = V(\Omega)\mathbf{x}_b(\Omega) = \frac{1}{3}\int_0^{2\pi} \left[\begin{smallmatrix} \cos\phi \\ \sin\phi \end{smallmatrix}\right] r^3(\phi) d\phi \tag{1.4}$$

simplifies the constraints.

Now we are able to define the three classes of optimization problems under consideration

$$\left.\begin{aligned} J(\Omega) = -B(\Omega) \to \min \quad & \text{subject to} \\ V(\Omega) \le V_0, \quad T(\Omega) \ge T_0, \quad & \widehat{\mathbf{x}}_b(\Omega) = \mathbf{0}, \end{aligned}\right\} \tag{P1}$$

$$\left.\begin{aligned} J(\Omega) = V(\Omega) \to \min \quad & \text{subject to} \\ B(\Omega) \ge B_0, \quad T(\Omega) \ge T_0, \quad & \widehat{\mathbf{x}}_b(\Omega) = \mathbf{0}, \end{aligned}\right\} \tag{P2}$$

and

$$\left.\begin{aligned} J(\Omega) = -T(\Omega) \to \min \quad & \text{subject to} \\ V(\Omega) \le V_0, \quad B(\Omega) \ge B_0, \quad & \widehat{\mathbf{x}}_b(\Omega) = \mathbf{0}. \end{aligned}\right\} \tag{P3}$$

In the sequel, we will mainly discuss the methods and transformations for (P1). At least from a technical point of view, the adaptions for the other problems are more or less along the lines. However, the solutions to these problems depend differently on the choice of the bounds for the inequality constraints, we refer to [2] for details. Furthermore, we observed a slightly different behaviour in the algorithms, which we will investigate later.

1.2. **Shape calculus and necessary condition.** We briefly recall well known facts about the first order shape calculus, useful for both, the discussion of necessary conditions and the numerical algorithms. For a well focussed introduction we refer to [29]. But in the case of our examples, also methods from a calculus of variation-like approach are applicable, cf. [1, 26]. For the adaption to polar coordinates one might use [14, 15]. As a consequence, we obtain the following formulas for related shape gradients, which denotes in fact a Fréchet-derivative,

$$\begin{aligned} \nabla V(r)[dr] &= \int_\Gamma \langle dr\mathbf{e}_r, \mathbf{n}\rangle d\sigma = \int_0^{2\pi} dr(\phi) r(\phi) d\phi, \\ \nabla B(r)[dr] &= \int_\Gamma \langle dr\mathbf{e}_r, \mathbf{n}\rangle y^2 d\sigma = \int_0^{2\pi} dr(\phi) \sin^2\phi\, r^3(\phi) d\phi, \\ \nabla \widehat{\mathbf{x}}_b(r)[dr] &= \int_\Gamma \langle dr\mathbf{e}_r, \mathbf{n}\rangle \mathbf{x} d\sigma = \int_0^{2\pi} dr(\phi) \left[\begin{smallmatrix}\cos\phi \\ \sin\phi\end{smallmatrix}\right] r^2(\phi) d\phi. \end{aligned} \tag{1.5}$$

For domain respective volume functionals, note that we always derive a boundary integral with the trace of the integrand times the normal component of the boundary variation as the shape gradient.

For the differentiation of the torsional rigidity we introduce the adjoint state $p = p(\Omega)$

$$\begin{aligned} -\Delta p &= 2 \quad \text{in } \Omega, \\ p &= 0 \quad \text{on } \Gamma, \end{aligned}$$

and the local shape derivative $du = du[dr]$ of the state in direction dr

$$\begin{aligned} -\Delta du[dr] &= 0 && \text{in } \Omega, \\ du[dr] &= -\langle dr\mathbf{e}_r, \mathbf{n}\rangle \tfrac{\partial u}{\partial \mathbf{n}} && \text{on } \Gamma. \end{aligned} \tag{1.6}$$

Therefore, the shape gradient of the torsional rigidity reads as follows

$$\begin{aligned} \nabla T(\Omega)[dr] &= \int_\Omega 2du[dr]d\mathbf{x} \\ &= \int_\Gamma \langle dr\mathbf{e}_r, \mathbf{n}\rangle \Big(\frac{\partial u}{\partial \mathbf{n}}\Big)^2 d\sigma \\ &= \int_0^{2\pi} dr(\phi) r(\phi) \Big(\frac{\partial u}{\partial \mathbf{n}}(\phi)\Big)^2 d\phi. \end{aligned} \tag{1.7}$$

Remark 1.2. *As an alternative approach one might use domain perturbation methods like the speed method or the perturbation of identity. The latter one is also called method of mappings. Due to the nature of this, domain integral representations of shape gradients occur directly. However, after standard transformations one derives equivalent boundary integrals which turn out completely analogous to the expressions presented above. In fact, provided that the domain itself is sufficiently smooth, the functionals arising from our problems have second and higher order shape derivatives* [13, 15, 29].

Now we are in a position to study the necessary condition for problem (P1). To that aim, we introduce the Lagrangian as usual

$$\begin{aligned} L(\Omega, \boldsymbol{\lambda}) &= B(\Omega) + \lambda_T\big(T(\Omega) - T_0\big) + \lambda_V\big(V(\Omega) - V_0\big) + \langle \boldsymbol{\lambda}_{\widehat{\mathbf{x}}_b}, \widehat{\mathbf{x}}_b\rangle \\ &= \int_\Omega -y^2 + \lambda_T u(\mathbf{x}) + \lambda_V + \langle \boldsymbol{\lambda}_{\widehat{\mathbf{x}}_b}, \mathbf{x}\rangle \, d\mathbf{x}, \end{aligned}$$

where $\boldsymbol{\lambda} = [\lambda_T, \lambda_V, \boldsymbol{\lambda}_{\widehat{\mathbf{x}}_b}^T]^T$. This yields the related shape gradient

$$\nabla L(\Omega, \boldsymbol{\lambda})[dr] = \int_\Gamma \langle dr\mathbf{e}_r, \mathbf{n}\rangle \Big\{ -y^2 + \lambda_V + \lambda_T \Big(\frac{\partial u}{\partial \mathbf{n}}\Big)^2 + \langle \boldsymbol{\lambda}_{\widehat{\mathbf{x}}_b}, \mathbf{x}\rangle \Big\} \, d\sigma.$$

Hence, we obtain a free problem with respect to the boundary variation dr, and by standard results we have the well known

Theorem 1.3 (Necessary first order optimality condition)**.** *Let $\Omega^\star$ be a regular optimal solution for problem (P1). Then, there exist $\lambda_V^\star \geq 0$ and $\lambda_T^\star \leq 0$ such that $\nabla L(\Omega^\star, \boldsymbol{\lambda}^\star)[dr] = 0$ for all dr. In other words, we have*

$$\Big\{ -y^2 + \lambda_V^\star + \lambda_T^\star \Big(\frac{\partial u}{\partial \mathbf{n}}\Big)^2 + \langle \boldsymbol{\lambda}_{\widehat{\mathbf{x}}_b}^\star, \mathbf{x}\rangle \Big\}\Big|_{\Gamma^\star} \equiv 0. \tag{1.8}$$

Additionally, $\Omega^\star$ satisfies in combination with $\boldsymbol{\lambda}^\star$ the complementary slackness conditions

$$\lambda_T^\star \big(T(\Omega) - T_0\big) = \lambda_V^\star \big(V(\Omega) - V_0\big) = \boldsymbol{\lambda}_{\widehat{\mathbf{x}}_b,x}^\star \widehat{x}_b(\Omega) = \boldsymbol{\lambda}_{\widehat{\mathbf{x}}_b,y}^\star \widehat{y}_b(\Omega) = 0.$$

Remark 1.4. *We do not have any type of convexity for the shape problem. Hence, to ensure a Kuhn-Tucker type condition, the regularity of $\Omega^\star$ is really an additional assumption which cannot be guaranteed in advance. Nevertheless, we will have regular stationary domains, see the next subsection.*

1.3. **Stationary shapes.** In the present subsection, we discuss the analytical solution of the necessary condition. For the sake of brevity, we restrict ourselves to the minimization problem (P1). Let us remark, that the discussion of the other problems is rather similar, cf. [2].

Theorem 1.5 (Banichuk/Karihaloo [2])**.** *Let T_0 and V_0 be given such that both constraints on the torsional rigidity and the volume are active. Then, the ellipse $\Omega^\star$ defined via $x^2 + ay^2 = b$, $a \leq 1$, fulfills the necessary conditions for*

$$b = \frac{V_0\sqrt{a}}{\pi}\,, \qquad \sqrt{a} = \frac{V_0^2 - \sqrt{V_0^4 - 4\pi^2 T_0^2}}{2\pi T_0}\,.$$

The Lagrange multipliers are given by

$$\lambda_V^\star = \frac{V_0}{\pi\sqrt{a}(1-a)}\,, \qquad \lambda_T^\star = -\frac{(1+a)^2}{4a(1-a)}\,, \qquad \boldsymbol{\lambda}_{\widehat{\mathbf{x}}_b}^\star = \mathbf{0}\,,$$

and the optimal value computes as

$$B(\Omega^\star) = \frac{\pi b^2}{4a^{3/2}}\,.$$

Proof. We briefly recall a fews steps from the proof in [2]. Let us consider an ellipse defined as above. From the ansatz for the stress function $u^\star = N(b - x^2 - ay^2)$ follows that $\Delta u^\star = -2(1+a)N$, that is $1/N = 1 + a$. We arrive at

$$\frac{\partial u^\star}{\partial \mathbf{n}} = -2N\sqrt{x^2 + a^2y^2} = -2\frac{\sqrt{b - a(1-a)y^2}}{1+a}\,,$$

and

$$T(\Omega^\star) = \frac{Nb^2\pi}{\sqrt{a}} = \frac{b^2\pi}{(1+a)\sqrt{a}}\,.$$

The formula for the volume is $V(\Omega^\star) = b\pi/\sqrt{a}$. Applying (1.8), the comparison of the coefficients together with the activity of the constraints yields a nonlinear system of equations for the appearing constants. This can be solved explicitly by the solution given above. □

Remark 1.6. 1. *In dependence from the ratio T_0/V_0 the optimization problem behaves different. For $T_0 > \frac{V_0^2}{2\pi}$ no admissible domain exists with respect to the constraints. For the limit case $T_0 = \frac{V_0^2}{2\pi}$ the once admissible domain is a circle with an appropriate radius. In the case $T_0 < \frac{V_0^2}{2\pi}$ we obtain an ellipse with semiaxes $h_x = \sqrt{b}$ and $h_y = \sqrt{b/a}$.*

2. *Assuming $V_0 = \pi$, we find the following asymptotic behaviour. Since $b = \sqrt{a}$, for $2T_0 \sim \pi - \varepsilon^2$ and $T_0 = \varepsilon$ we conclude that $\sqrt{a} \sim 1 - \frac{2\varepsilon}{\pi}$ and $\sqrt{a} \sim \frac{\varepsilon}{\pi}$, respectively, if $\varepsilon \to 0$. This implies $\lambda_V^\star \to \infty$ and $\lambda_T^\star \to -\infty$.*

3. *As mentioned above, the discussion for the problems (P2) and (P3) is very similar. However, by varying the values for the bounds we find admissible domains for all given values of the bounds. Nevertheless, for some ratios B_0/T_0 and V_0/B_0, respectively, the bending constraint is oversatisfied and the stationary solution provides the circle as optimum, see* [3, 13].

Remark 1.7. *In the context of general classes of C^2-domains, the calculus is completely valid in the neighbourhood of the stationary solutions. This results from the fact that every regular starshaped domain has an open C^2-neighbourhood which contains only starshaped domains. We find even that the strict convexity of the ellipse*

$$\frac{h_x}{h_y^2} = \kappa_{\min} \le \kappa \le \kappa_{\max} = \frac{h_y}{h_x^2},$$

implies a C^2-neighbourhood containing only strictly convex domains.

Remark 1.8. *According to $\mathbf{e}_r = \mathbf{x}/\|\mathbf{x}\|$, we find*

$$\langle \mathbf{e}_r, \mathbf{n} \rangle = \frac{x^2 + ay^2}{\sqrt{(x^2+y^2)(x^2+a^2y^2)}} = \frac{b}{\sqrt{(x^2+y^2)(x^2+a^2y^2)}}\,.$$

and, for $\mathbf{x} = \mathbf{x}(\phi) \in \Gamma^\star$,

$$\mathbf{x}(\phi) = \frac{\sqrt[4]{a}}{\sqrt{\cos^2\phi + a\sin^2\phi}}\mathbf{e}_r(\phi).$$

Hence, even at $\Omega^\star$, the local shape derivative $du^\star[dr]$ satisfies the Dirichlet boundary condition

$$du^\star[dr]\big(\mathbf{x}(\phi)\big) = \frac{2\sqrt{a}dr(\phi)}{(1+a)\sqrt{x(\phi)^2 + y(\phi)^2}},$$

cf. (1.6). *This condition is not of the type constant times the boundary variation* dr. *Hence, in contrast to the examples in* [3], *there exists no explicit representation of the local shape derivative* $du^\star[dr]$ *by power or Fourier series.*

2. Approximation for the shapes and optimization algorithms

2.1. **Finite dimensional representation of boundaries.** There are some difficulties in treating the shape problems analogously to usual control problems in infinite dimensional spaces.

- The discussion of descent methods of first order causes trouble even if the class of shapes under consideration can be identified with elements of a Banach space X like in our approach. In fact, this needs a reinterpretation of gradients as elements of $X^\star$ in the space X. However, a shape differential calculus often works in a canonical way in spaces having a "complicated dual", for example $C^2_{\rm per}([0, 2\pi])$ in our case, cf. (0.1). An embedding in a Hilbert space is difficult, too. Moreover, the gradient of a wide class of objectives is given with respect to a L_2-duality. This requires the application of an additional duality mapping.

- The state $u = u(\Omega)$ lives in a domain-dependent functional space. This causes the boundary value problem not treatable straightforward as an equality constraint which is well defined via a mapping between Banach spaces. Usually u is inserted into the objective and the shape differentiation is performed by the chain rule via the material or local shape derivative concept for the state [14, 25, 29].

Due to these difficulties, we proceed our paper as follows. First, we discuss a finite dimensional approximation *only* for the shapes. Necessarily, it has to be compatible with a related approximation for the shape gradients. Second, we consider all shape functionals as exactly computable. This includes the computation of the torsional rigidity via the stress function. Proceeding that way, we derive a finite dimensional constraint optimization problem without having any trouble for performing gradient or Quasi-Newton steps.

The approximation of the stress function is considered *independently* from the shape approximation. As an immediate consequence, the related discretization is decoupled from the finite dimensional subspace of the shapes. It is worth noting that the restriction to a finite dimensional optimization problem induces the investigation of convergence. But this will not considered in the present paper.

Based on the polar coordinate approach, we can express the smooth function $r \in C^2_{\mathrm{per}}([0, 2\pi])$ by

$$r(\phi) = a_0 + \sum_{n=1}^{\infty} a_n \cos n\phi + a_{-n} \sin n\phi.$$

Hence, it is obvious to take the truncated Fourier series

$$r_N(\phi) = a_0 + \sum_{n=1}^{N} a_n \cos n\phi + a_{-n} \sin n\phi.$$

as approximation of r.

The advantages of this approach is an exponential convergence if the shape is analytical, i.e.,

$$|(r - r_N)(\phi)| \lesssim q^N \tag{2.9}$$

for an appropriate $q < 1$. In fact, the ellipses arising from our optimization problems are analytical as well. Additoinally, the approximation r_N is analytical which makes the application of the wavelet Galerkin scheme for the boundary element method much more efficient [23].

The finite dimensional approximation of the shape gradient is given via the coefficients of the finite Fourier series to the trace function of the related boundary integral representation. That is, for any given domain functional $J(\Omega) = \int_\Omega j(\mathbf{x}) d\mathbf{x}$, the shape gradient

$$\nabla J(\Omega)[dr] = \int_0^{2\pi} dr(\phi) \cdot (r(\phi) j(\phi))\, d\phi$$

is approximated by

$$\nabla_N J(\Omega) := \int_0^{2\pi} \begin{bmatrix} \sin N\phi \\ \sin(N-1)\phi \\ \vdots \\ \cos N\phi \end{bmatrix} \cdot (r(\phi) j(\phi))\, d\phi.$$

Remark 2.1. *According to remark 1.2, our approach ensures that the higher order smoothness of the original problems is passed on the finite dimensional subproblems. Obviously, this is not essential for the realization of first order optimization methods. However, it is indispensible for the investigation of the convergence of the algorithms in the finite dimensional setting.*

2.2. **Relaxation of the constraints.** The crucial idea for the numerical algorithms is the transformation of the problems (P1), (P2) and (P3) to unconstrained optimization problems. In particular, we treat the applicability of well developed standard

techniques which involve only gradient informations. For the sake of brevity, we restrict ourselves to problem (P1). The corresponding formulations of the problems (P2) and (P3) is given completely analogous.

The simplest formulation makes use of a quadratic *penalty functional*

$$P_\alpha(\Omega) = -B(\Omega) + \frac{\alpha}{2}\Big[\big(\min\{0, T(\Omega) - T_0\}\big)^2 + \big(\max\{0, V(\Omega) - V_0\}\big)^2 + \|\widehat{\mathbf{x}}_b(\Omega)\|^2\Big]. \tag{2.10}$$

The main advantage is a *simultaneous* handling of equality and active/nonactive inequality constraints. However, ensuring smoothness *and* convergence requires formally $\alpha \to \infty$ during the iteration process. Usually, the problems become ill conditioned for large α.

At least in the case of active constraints, the *Augmented Lagrangian* for equailty constraints offers a more stable formulation

$$L_c^e(\Omega, \boldsymbol{\lambda}) = -B(\Omega) + \lambda_T\big(T(\Omega) - T_0\big) + \lambda_V\big(V(\Omega) - V_0\big) + \langle \lambda_{\widehat{\mathbf{x}}_b}, \widehat{\mathbf{x}}_b(\Omega)\rangle + \frac{c}{2}\Big[\big(T(\Omega) - T_0\big)^2 + \big(V(\Omega) - V_0\big)^2 + \|\hat{x}_S(\Omega)\|^2\Big]. \tag{2.11}$$

Here we have the following update for the Lagrange multiplier

$$\boldsymbol{\lambda}_{k+1} = \boldsymbol{\lambda}_k + c \begin{bmatrix} T_0 - T(\Omega_k) \\ V_0 - V(\Omega_k) \\ \widehat{\mathbf{x}}_b(\Omega_k) \end{bmatrix} \quad \longrightarrow \quad \boldsymbol{\lambda}^\star,$$

where c is fixed but appropriately chosen.

Remark 2.2. *The literature offers a lot of adaptions of the Augmented Lagrangian or modified Lagrangian techniques for the inequality constraints as well as for a moderate change of the penalty-like parameter c. Nevertheless, like the quadratic penalty functional, the Augmented Lagrangian L_c^i for inequality constraints is only $C^{1,1}$ even for a smooth original problem. This might cause problems in view of higher order methods or a refined treatment of convergence.*

For further details on the theory of penalty methods and the Augmented Lagrangian we refer to [16, 19, 27] and the references therein. We mention that we do not treat the pure Lagrange method since it is known too slow and not robust enough, cf. [16, 19].

2.3. **Descent methods of first order.** For the minimization of the auxiliary problems (2.10) and (2.11) we apply the gradient method, also known as steepest descent. Whereas this method is simple to implement, the convergence is known rather poor. In contrary, under suitable conditions, the class of Quasi-Newton methods ensures

Penalty algorithm

- starting point: Choose initial guess r_0, choose $\alpha_0, \varepsilon_0^{(1)}, \varepsilon_0^{(2)}, q \in (0,1)$.
- outer iteration: For iteration index $i = 1, 2, \ldots$ update

$$\alpha_i = \alpha_{i-1} + c, \quad c > 0,$$

  and solve $\min P_{\alpha_i}(r)$ with initial guess $r_i^0 := r_{i-1}$.
- inner iteration: For iteration index $j = 1, 2, \ldots$ update

$$r_i^j = r_i^{j-1} + \delta h_i^{j-1},$$

  with descent direction h_i^{j-1} and δ from line search.
- line search: Set $\delta := 1$.
  While $P_{\alpha_i}(r_i^{j-1} + \delta h_i^{j-1}) \geq P_{\alpha_i}(r_i^{j-1}) + q\delta \nabla P_{\alpha_i}(r_i^{j-1})[h_i^{j-1}]$ do

$$\delta := \frac{\frac{1}{2}\nabla P_{\alpha_i}(r_i^{j-1})[h_i^{j-1}]}{\nabla P_{\alpha_i}(r_i^{j-1})[h_i^{j-1}] + P_{\alpha_i}(r_i^{j-1} + \delta h_i^{j-1}) - P_{\alpha_i}(r_i^{j-1})}\,.$$

- stopping criterion: Either

$$0 < \frac{P_{\alpha_i}(r_i^{j-1}) - P_{\alpha_i}(r_i^j)}{|P_{\alpha_i}(r_i^{j-1})|} < \varepsilon_i^{(1)}, \qquad \varepsilon_i^{(1)} = q\varepsilon_{i-1}^{(1)},$$

  or/and

$$\|\nabla P_{\alpha_i}(r_i^j)\| \leq \varepsilon_i^{(2)}, \qquad \varepsilon_i^{(2)} = q\varepsilon_{i-1}^{(2)}.$$

FIGURE 2.1. A principal optimization algorithm.

superlinear convergence via a local approximation of the Hessian in the descent direction. Hence, additionally we consider one representative using a special version of inverse BFGS-rule.

For instance, for the penalty functional these methods are given as follows.

- *Gradient method:* The descent direction is the anti-gradient

$$\mathbf{d}_{k+1} = -\nabla_N P_\alpha(\Omega_k).$$

- *Quasi-Newton method:* The descent direction is given by

$$\mathbf{d}_{k+1} = -\mathbf{H}_k \nabla_N P_\alpha(\Omega_k),$$

  where $\mathbf{H}_k$ is updated by the inverse BFGS-rule without damping.

We skip the discussion of the structure and properties of the various kinds of Quasi-Newton update rules found in the literature. For further update rules and their theory of convergence we refer to [11, 12, 17, 19].

For the sake of completeness, we present an algorithmical scheme in figure 2.1. We formulate it with respect to the penalty functional. In particular, a second order approximation is proposed for performing the line search update if a descent fails. Clearly, it is also applicable for the Quasi-Newton method.

3. Solving the Partial Differential Equation

3.1. **Boundary integral formulation.** In order to evaluate the data arising from the torsional rigidity $T(\Omega)$ (1.2) and its shape gradient $\nabla T(\Omega)[dr]$ (1.7), we require $\int_\Omega u \, d\mathbf{x}$ and the normal derivative $\frac{\partial u}{\partial \mathbf{n}}$ with respect to the solution u of the boundary value problem (1.3). Without loss of generality we assume the domain Ω arbitrarily but fixed and sufficiently smooth in this section.

We simplify the evaluation of $\int_\Omega u \, d\mathbf{x}$ by making use of the second Green formula

$$\int_\Omega u\Delta q \, d\mathbf{x} = \int_\Omega \Delta u q \, d\mathbf{x} + \int_\Gamma u\frac{\partial q}{\partial \mathbf{n}} \, d\sigma - \int_\Gamma \frac{\partial u}{\partial \mathbf{n}} q \, d\sigma.$$

Setting $q(\mathbf{x}) := \frac{1}{4}(x^2 + y^2)$ and observing $\Delta u = -2$, $u\big|_\Gamma = 0$ as well as $\Delta q = 1$, we derive the equation

$$\int_\Omega u d\mathbf{x} = \int_\Omega u\Delta q d\mathbf{x} = -2\int_\Omega q d\mathbf{x} - \int_\Gamma \frac{\partial u}{\partial \mathbf{n}} q d\sigma. \tag{3.12}$$

According to

$$\int_\Omega q d\mathbf{x} = \int_0^{2\pi}\int_0^{r(\phi)} q(\rho,\phi)\rho d\rho d\phi = \frac{1}{16}\int_0^{2\pi} r(\phi)^4 d\phi,$$

the first integral on the right hand side of (3.12) can be calculated cheaply by a boundary integral. Hence, it suffices to compute the normal derivative of the stress function.

The Newton potential $v(\mathbf{x}) := -\frac{1}{2}(x^2 + y^2)$ satisfies the equation $\Delta v = -2$. Hence, making the ansatz

$$u := v + w, \tag{3.13}$$

a harmonical function w is sought which satisfies the boundary value problem

$$\begin{aligned} \Delta w &= 0 \quad && \text{in } \Omega, \\ w &= -v \quad && \text{on } \Gamma. \end{aligned} \tag{3.14}$$

The latter problem can be solved by a boundary integral equation. We introduce the *single layer operator* $\mathcal{V}$ and the *double layer operator* $\mathcal{K}$ defined by

$$(\mathcal{V}u)(\mathbf{x}) := -\frac{1}{2\pi}\int_\Gamma \log\|\mathbf{x}-\mathbf{y}\|u(\mathbf{y})d\sigma_\mathbf{y},$$
$$(\mathcal{K}u)(\mathbf{x}) := \frac{1}{2\pi}\int_\Gamma \frac{\langle \mathbf{n}_\mathbf{y}, \mathbf{x}-\mathbf{y}\rangle}{\|\mathbf{x}-\mathbf{y}\|^2}u(\mathbf{y})d\sigma_\mathbf{y}.$$

Then, the normal derivative $\omega := \frac{\partial w}{\partial \mathbf{n}}$ is given by the Dirichlet-to-Neumann map

$$\mathcal{V}\omega = \Big(\frac{1}{2}+\mathcal{K}\Big)w \quad \text{on } \Gamma. \tag{3.15}$$

We denote the function space of all squared integrable functions on Γ with respect to the canonical inner product

$$(u,v)_{L^2(\Gamma)} = \int_\Gamma uv\, d\sigma$$

by $L^2(\Gamma)$ and the associated Sobolev spaces by $H^s(\Gamma)$, $s\in\mathbb{R}$. Then, in this context, $\mathcal{V}: H^{-1/2}(\Gamma)\to H^{1/2}(\Gamma)$ defines an operator of the order -1 while $\frac{1}{2}+\mathcal{K}: H^{1/2}(\Gamma)\to H^{1/2}(\Gamma)$ defines an operator of the order 0.

Remark 3.1. *The above proceeding is feasible for a general class of problems. On the one hand, different inhomogenities in* (1.3) *can be treated if appropriate Newton potentials are known. On the other hand, the homogeneous Dirichlet data are not essential for our approach.*

3.2. **The Galerkin scheme.** We employ a Galerkin scheme in order to discretize (3.15). Exploiting polar coordinates, we introduce a parametrical representation of the boundary in accordance with

$$\gamma:[0,1]\to\Gamma,\quad s\mapsto\gamma(s) := r(2\pi s)\left[\begin{smallmatrix}\cos(2\pi s)\\ \sin(2\pi s)\end{smallmatrix}\right].$$

We subdivide the boundary Γ into 2^l panels $\pi_{l,k} := \gamma\big(2^{-l}[k,k+1)\big)$, $k\in\triangle_l := \{0,1,\dots,2^l-1\}$. With respect to this partition, the piecewise constants $\Phi_l^{(1)} := \{\phi_{l,k}^{(1)} : k\in\triangle_l\}$ and linears $\Phi_l^{(2)} := \{\phi_{l,k}^{(2)} : k\in\triangle_l\}$ are given by

$$\phi_{l,k}^{(1)} = 2^{l/2}\chi_{\pi_{l,k}}$$

and

$$\phi_{l,k}^{(2)}(\mathbf{x}) = 2^{3l/2}\begin{cases} s-2^{-l}(k-1), & \mathbf{x}=\gamma(s)\in\pi_{l,k-1},\\ 2^{-l}(k+1)-s, & \mathbf{x}=\gamma(s)\in\pi_{l,k},\\ 0, & \text{elsewhere,}\end{cases}$$

respectively. Note that we use a L^2-normalization, i.e., $\|\phi_{l,k}^{(d)}\|_{L^2(\Gamma)}\sim 1$ for $d=1,2$.

Making the ansatz $\omega_l = \Phi_l^{(1)} \boldsymbol{\omega}_l^\phi$ we have to solve the Galerkin system

$$\mathbf{V}_l^\phi \boldsymbol{\omega}_l^\phi = \big((\tfrac{1}{2} + \mathcal{K}) w, \Phi_l^{(1)} \big)_{L^2(\Gamma)} \tag{3.16}$$

with the system matrix

$$\mathbf{V}_l^\phi := (\mathcal{V} \Phi_l^{(1)}, \Phi_l^{(1)})_{L^2(\Gamma)}.$$

For the application of the wavelet matrix compression, we approximate the given Dirichlet data in (3.14) by piecewise linears. Its best approximation w_l with respect to $L^2(\Gamma)$ is given by

$$w_l := \Phi_l^{(2)} \big(\mathbf{G}_l^\phi \big)^{-1} \mathbf{w}_l^\phi$$

where

$$\mathbf{G}_l^\phi := (\Phi_l^{(2)}, \Phi_l^{(2)})_{L^2(\Gamma)}, \quad \mathbf{w}_l^\phi := (w, \Phi_l^{(2)})_{L^2(\Gamma)}.$$

Inserting this approximation into the Galerkin system (3.16) yields

$$\mathbf{V}_l^\phi \boldsymbol{\omega}_l^\phi = \big(\tfrac{1}{2} \mathbf{B}_l^\phi + \mathbf{K}_l^\phi \big) \big(\mathbf{G}_l^\phi \big)^{-1} \mathbf{w}_l^\phi \tag{3.17}$$

with

$$\mathbf{B}_l^\phi := (\Phi_l^{(2)}, \Phi_l^{(1)})_{L^2(\Gamma)}, \quad \mathbf{K}_l^\phi := (\mathcal{K} \Phi_l^{(2)}, \Phi_l^{(1)})_{L^2(\Gamma)}.$$

We mention that the approximation by piecewise linears is required in order to get the optimal order of convergence of the Galerkin scheme.

3.3. **Wavelet approximation for BEM.** The system matrices $\mathbf{V}_l^\phi$ and $\mathbf{K}_l^\phi$ are densely populated. In combination with the ill-posedness of $\mathbf{V}_l^\phi$, this implies at least a quadratic complexity for the computation of the Neumann data ω_l^ϕ. Instead of using the *single-scale bases* for the discretization, we apply biorthogonal wavelet bases and compress the arising system matrices.

More precisely, defining $V_l^{(d)} := \operatorname{span} \Phi_l^{(d)}$, the two sequences of nested spaces

$$V_{l_0}^{(d)} \subset V_{l_0+1}^{(d)} \subset \dots, \quad \operatorname{clos}_{L^2(\Gamma)} \Big(\bigcup_{l \geq l_0} V_l^{(d)} \Big) = L^2(\Gamma), \quad \bigcap_{l \geq l_0} V_l^{(d)} = V_{l_0}^{(d)},$$

generate a multiscale analysis, cf. [5]. We introduce suitable wavelet bases $\Psi_l^{(d)} := \{ \psi_{l,k}^{(d)} : k \in \triangle_l \}$ which span complementary spaces $W_l^{(d)} := \operatorname{span} \Psi_l^{(d)}$ with

$$V_l^{(d)} \oplus W_l^{(d)} = V_{l+1}^{(d)}.$$

For the matrix compression, these wavelet bases are required to have vanishing moments in terms of

$$\int_\Gamma \big(\gamma^{-1}(\mathbf{x}) \big)^\alpha \psi_{l,k}^{(d)}(\mathbf{x}) d\sigma = 0, \quad 0 \leq \alpha < \widetilde{d}.$$

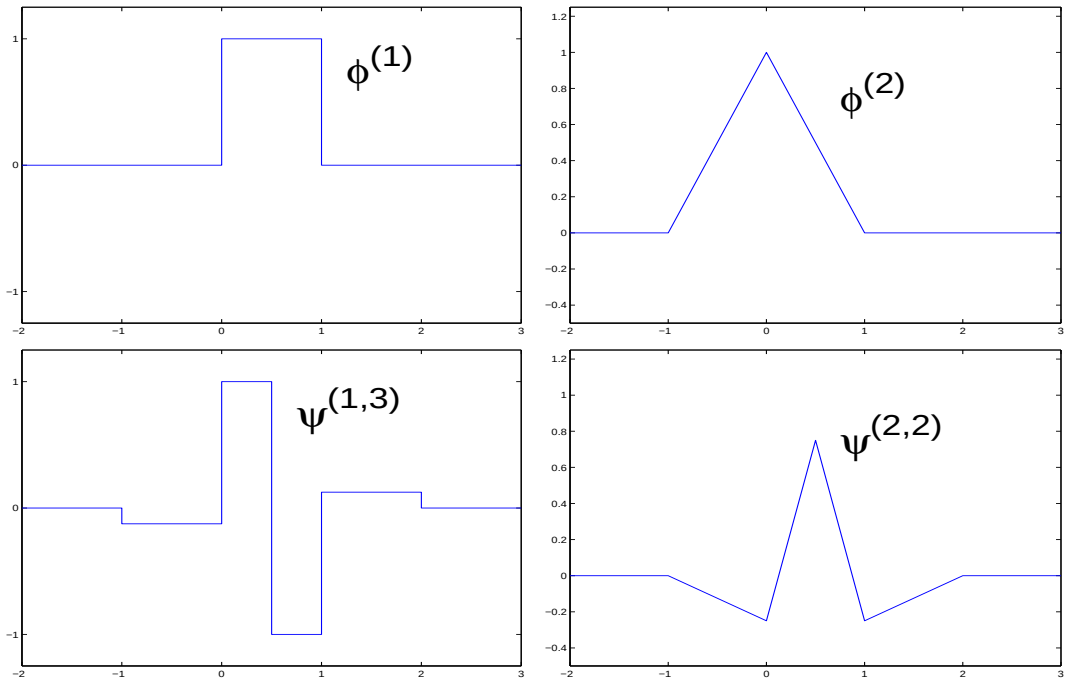

FIGURE 3.2. Piecewise constant and linear functions respective wavelets

According to [21, 22], it suffices to consider piecewise constant wavelets with $\widetilde{d} = 3$ vanishing moments and piecewise linear wavelets with $\widetilde{d} = 2$ vanishing moments. Such wavelets have been constructed in [5]. They can be described by their refinement relation

$$\psi_{l,k}^{(d)} = \sum_j a_j \phi_{l+1,2k+j}^{(d)}$$

with the *mask coefficients*

$$(a_{-2}, a_{-1}, \dots, a_3) = (-1/8, -1/8, 1, -1, 1/8, 1/8), \qquad d = 1,$$
$$(a_{-1}, a_0, \dots, a_3) = (-1/8, -1/4, 3/4, -1/4, -1/8), \quad d = 2,$$

cf. figure 3.2. It is well known [5] that the collections

$$\Psi_L^{(d)} := \bigcup_{l=l_0-1}^{L} \Psi_l^{(d)},$$

with $\Psi_{l_0-1}^{(d)} := \Phi_{l_0}^{(d)}$ form uniformly stable bases in $L^2(\Gamma)$. In fact, this *Riesz property* implies the existence of a corresponding *dual* multiresolution analysis. We refer to [5, 23, 28] for details.

Now, replacing $\Phi_L^{(d)}$ by $\Psi_L^{(d)}$ in (3.17), we obtain the wavelet Galerkin system

$$\mathbf{V}_L^{\psi} \boldsymbol{\omega}_L^{\psi} = \left(\tfrac{1}{2}\mathbf{B}_L^{\psi} + \mathbf{K}_L^{\psi}\right)\left(\mathbf{G}_L^{\psi}\right)^{-1} \mathbf{w}_L^{\psi} \tag{3.18}$$

with

$$\mathbf{V}_L^\psi := (\mathcal{V}\Psi_L^{(1)}, \Psi_L^{(1)})_{L^2(\Gamma)}, \quad \mathbf{K}_L^\psi := (\mathcal{K}\Psi_L^{(2)}, \Psi_L^{(1)})_{L^2(\Gamma)},$$
$$\mathbf{B}_L^\psi := (\Psi_L^{(2)}, \Psi_L^{(1)})_{L^2(\Gamma)}, \quad \mathbf{G}_L^\psi := (\Psi_L^{(2)}, \Psi_L^{(2)})_{L^2(\Gamma)},$$
$$\mathbf{u}_L^\psi := (w, \Psi_L^{(2)})_{L^2(\Gamma)}, \quad \omega_L := \Psi_L^{(1)}\boldsymbol{\omega}_L^\psi.$$

Herein, the system matrices $\mathbf{V}_L^\psi$ and $\mathbf{K}_L^\psi$ are quasi-sparse. Both matrices can be compressed without loss of accuracy to $\mathcal{O}(2^L)$ nonvanishing matrix entries, see [7, 21, 23, 28] for details. Actually, in accordance with [7, 23], the over-all complexity of compressing and assembling the system matrices is $\mathcal{O}(2^L)$. Moreover, based on the well known norm equivalences of wavelet bases, $\operatorname{diag}(\mathbf{V}_L^\psi)$ provides an simple preconditioner of the system matrix corresponding to the single layer operator [6, 8, 10, 28].

Observing that the single-scale matrix $\mathbf{G}_L^\phi$ and the wavelet matrix $\mathbf{G}_L^\psi$ are related by a wavelet transform $\mathbf{G}_L^\psi = \mathbf{T}_L\mathbf{G}_L^\phi\mathbf{T}_L^\star$, we deduce $(\mathbf{G}_L^\psi)^{-1} = \mathbf{T}_L^{-\star}(\mathbf{G}_L^\phi)^{-1}\mathbf{T}_L^{-1}$. Herein, the solution of the system $\mathbf{G}_L^\phi\mathbf{x} = \mathbf{y}$ requires only $\mathcal{O}(2^J)$ operations due to the bandedness of the piecewise linear mass matrix $\mathbf{G}_L^\phi$. Hence, the computation of the Neumann data ω_L^ψ has optimal complexity since the application of $\mathbf{T}_L^{-\star}$ and $\mathbf{T}_L^{-1}$ to a given vector scales also linearly (*fast wavelet transform*).

3.4. **Error estimates.** In this subsection we discuss the approximation errors of our approach. With respect to the normal derivative, we obtain the error estimate

$$\|\omega - \omega_L\|_{H^s(\Gamma)} \lesssim 2^{L(t-s)}\|\omega\|_{H^t(\Gamma)} \tag{3.19}$$

for all $-2 \le s \le t \le 1$, cf. [28].

Lemma 3.2. *The torsional rigidity T and its directional derivative $\nabla T[dr]$ are approximated cubic and quadratic with respect to the step width $h_L := 2^{-L}$, respectively. That is*

$$\big|T - T_L\big| \lesssim h_L^3, \qquad \big|(\nabla T - \nabla T_L)[dr]\big| \lesssim h_L^2. \tag{3.20}$$

Proof. First, we consider the discretization error for the torsional rigidity. Observing (3.12) and (3.13), we find the equation

$$\big|T - T_L\big| = \left|2\int_\Gamma \Big(\frac{\partial v}{\partial \mathbf{n}} + \omega\Big)d\sigma - 2\int_\Gamma \Big(\frac{\partial v}{\partial \mathbf{n}} + \omega_L\Big)d\sigma\right| = 2\big|(\omega - \omega_L, 1)_{L^2(\Gamma)}\big|.$$

Hence, invoking (3.19) we conclude

$$\big|T - T_L\big| \le 2\|\omega - \omega_L\|_{H^{-2}(\Gamma)}\|1\|_{H^2(\Gamma)} \lesssim 2^{-3L}\|\omega\|_{H^1(\Gamma)}.$$

Next, we estimate the error with respect to the directional derivative of the torsional rigidity. We find

$$\begin{aligned}\big|(\nabla T - \nabla T_L)[dr]\big| &= \left| \int_0^{2\pi} r dr \Big(\frac{\partial v}{\partial \mathbf{n}} + \omega\Big)^2 d\phi - \int_0^{2\pi} r dr \Big(\frac{\partial v}{\partial \mathbf{n}} + \omega_L\Big)^2 d\phi \right| \\ &\leq 2\Big|\big(r dr \tfrac{\partial v}{\partial \mathbf{n}}, \omega - \omega_L\big)_{L^2([0,2\pi])}\Big| + \Big|\big(r dr, \omega^2 - \omega_L^2\big)_{L^2([0,2\pi])}\Big|.\end{aligned}$$

The first term is estimated by

$$\begin{aligned}\Big|\big(r dr \tfrac{\partial v}{\partial \mathbf{n}}, \omega - \omega_L\big)_{L^2([0,2\pi])}\Big| &\leq \big\|r dr \tfrac{\partial v}{\partial \mathbf{n}}\big\|_{H^1([0,2\pi])} \|\omega - \omega_L\|_{H^{-1}([0,2\pi])} \\ &\lesssim 2^{-2L} \big\|r dr \tfrac{\partial v}{\partial \mathbf{n}}\big\|_{H^1([0,2\pi])} \|\omega\|_{H^1(\Gamma)}\end{aligned}$$

since $\|\cdot\|_{H^s(\Gamma)} \sim \|\cdot\|_{H^s([0,2\pi])}$ for all $s \in \mathbb{R}$ if γ is smooth. With respect to the second term, we find

$$\begin{aligned}&\Big|\big(r dr, \omega^2 - \omega_L^2\big)_{L^2([0,2\pi])}\Big| \\ &\quad\leq \max_{\phi\in[0,2\pi]} \big\{r(\phi) dr(\phi)\big\} \Big|\big(\omega - \omega_L, \omega + \omega_L\big)_{L^2([0,2\pi])}\Big| \\ &\quad= \max_{\phi\in[0,2\pi]} \big\{r(\phi) dr(\phi)\big\} \Big|(\omega - \omega_L, \omega - \omega_L)_{L^2([0,2\pi])} - 2\big(\omega, \omega - \omega_L\big)_{L^2([0,2\pi])}\Big| \\ &\quad\leq \max_{\phi\in[0,2\pi]} \big\{r(\phi) dr(\phi)\big\} \Big[\|\omega - \omega_L\|^2_{L^2([0,2\pi])} + 2\|\omega\|_{H^1([0,2\pi])} \|\omega - \omega_L\|_{H^{-1}([0,2\pi])}\Big] \\ &\quad\lesssim 2^{-2L} \Big[3 \max_{\phi\in[0,2\pi]} \big\{r(\phi) dr(\phi)\big\} \|\omega\|^2_{H^1(\Gamma)}\Big].\end{aligned}$$

This proves the assertion. □

Remark 3.3. *One requires $\mathcal{O}(2^{2L})$ triangles for the discretization of the domain in order to ensure the step width h_L. Hence, the complexity of globally continuous linear finite elements is $\mathcal{O}(2^{2L})$ while we find the asymptotics $\big|T - T_L\big| \lesssim h_L^2$ and $\big|(\nabla T - \nabla T_L)[dr]\big| \lesssim h_L$.*

4. Numerical results

In this section, we report the experiences from our numerical experiments. With respect to the given problems, we investigate the behaviour of the presented algorithms for various choices of the bounds of the constraints.

An overview of the behaviour of the algorithms is tabulated in table 4.1. It turns out that the Augmented Lagrangian is more robust and more accurate in comparison with the penalty functional. In particular, the penalty algorithm is divergent with respect to problem (P1). However, we observe that the convergence depends on the ratio h_y/h_x of the semiaxis of the stationary ellipse. Roughly spoken, the algorithms are convergent for randomly generated initial guesses if $h_y/h_x \in [1, 2]$. Starting with

nearly optimal shapes the convergence is extended to the range $h_y/h_x \in [2,3]$. But the algorithms do not find the optimimum for $h_y/h_x > 3$.

Remark 4.1. *The behaviour of penalty functional of the problem (P1) differs crucially from those of the problems (P2) and (P3). Namely, for all finite values α holds*

$$\inf\{P_\alpha(\Omega) : V(\Omega) = V_0,\ \widehat{\mathbf{x}}_b(\Omega) = \mathbf{0}\} = -\infty.$$

This is readily verified by considering a concentric ellipse with constant volume V_0 where the ratio of the semiaxes h_y/h_x increases to ∞. Whereas this is not a complete proof it illustrates the difficulties of the penalty approach for problem (P1).

	(P1)	(P2)	(P3)
Penalty functional	○	•	•
Augmented Lagragian	•	•	•
$h_y/h_x \in [1,2]$	random start domain		
$h_y/h_x \in [2,3]$	good initial guess		
$h_y/h_x > 3$	no convergence		

TABLE 4.1. Comparison of the applicability and behaviour of the algorithms for the different problems.

Table 4.2 is concerned with the comparison Quasi-Newton method versus gradient method. To that aim we choose $N = 16$ and $L = 8$, respectively. We iterate 20 times the penalty functional for problem (P2) applying the Quasi-Newton descent. This leads to the l^2-difference 0.025 between the approximated and the exact Fourier-coefficients. The gradient method requires more than three times the number of iterations in order to attain this accuracy. Due to the line search, the cpu-time increases even by a factor close to five.

penalty functional for (P2)	Quasi-Newton method	gradient method
number of iterations	20	64
l^2-error of Fourier coefficients	0.025	0.025
cpu-time in sec.	32	151

TABLE 4.2. Comparison of Quasi-Newton method vs. gradient method.

Remark 4.2. *We observe the convergence of the Lagrange multipliers $\boldsymbol{\lambda} \to \boldsymbol{\lambda}^\star$ for the Augmented Lagrangian. In particular, $\lambda_{\widehat{\mathbf{x}}_b} = \mathbf{0}$ is found also by our numerical experiments. As a consequence, strict complementarity holds not for the problems (P1), (P2) and (P3). Nevertheless, linear indepedence of the gradients of the active constraints might be satisfied at $\Omega^\star$ as it is known from* [3, 15].

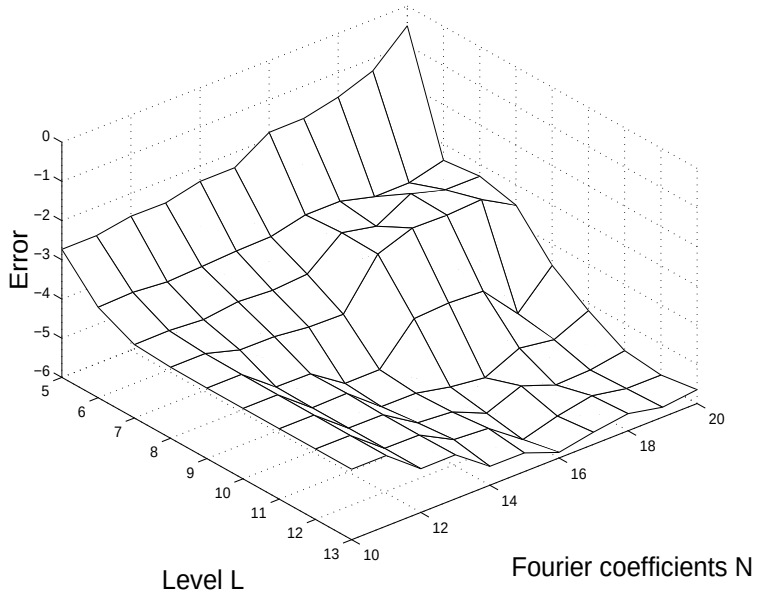

FIGURE 4.3. The l^2-error of the Fourier coefficients vs. the number of unknowns N_r and L.

Next, we investigate the error of approximation. We solve the optimization problem (P2) by using the Quasi-Newton method for the Augmented Lagrangian. We meassure the l^2-difference between the computed and the exact Fourier coefficients in dependance of the length N of the Fourier series and the number of boundary elements 2^L. Figure 4.3 shows this difference with respect to a $\log_{10}$-scale for all $10 \leq N \leq 20$ and $5 \leq L \leq 13$. It turns out that, for N fixed and L increasing, the error decreases up to a certain threshold. We suggest that this threshold is induced by the error of approximation of r_N (2.9) since it depends on N. On the other hand, for a fixed level L of discretization of the stress function, more Fourier coefficients seem first to improve and then to deteriorate of the error. Clearly, the improvement is realized by the higher power of approximation of r_N. The deterioration might be caused by oscillations of r_N which cannot be resolved by the number of boundary elements. Summarized one concludes that N and L should increase simultaneously, i.e., $N \sim L$. This observation seems to arise naturally from the orders of convergence (2.9) and (3.20).

A part of a iteration is specified in figure 4.4. We plot the domains obtained in the first 20 steps of the optimization of the penalty functional for problem (P2) where the descent is computed via the Quasi-Newton method. We choose $N = 16$ and 256 boundary elements while the penalty $\alpha = 5$ is fixed. The computation requires 45 sec. We emphasize that not only the presented domains are computed. In the most steps also the line search is active. In the 20th step, the l^2-distance of the approximated Fourier-coefficients to those of the optimal ellipse is 0.032.

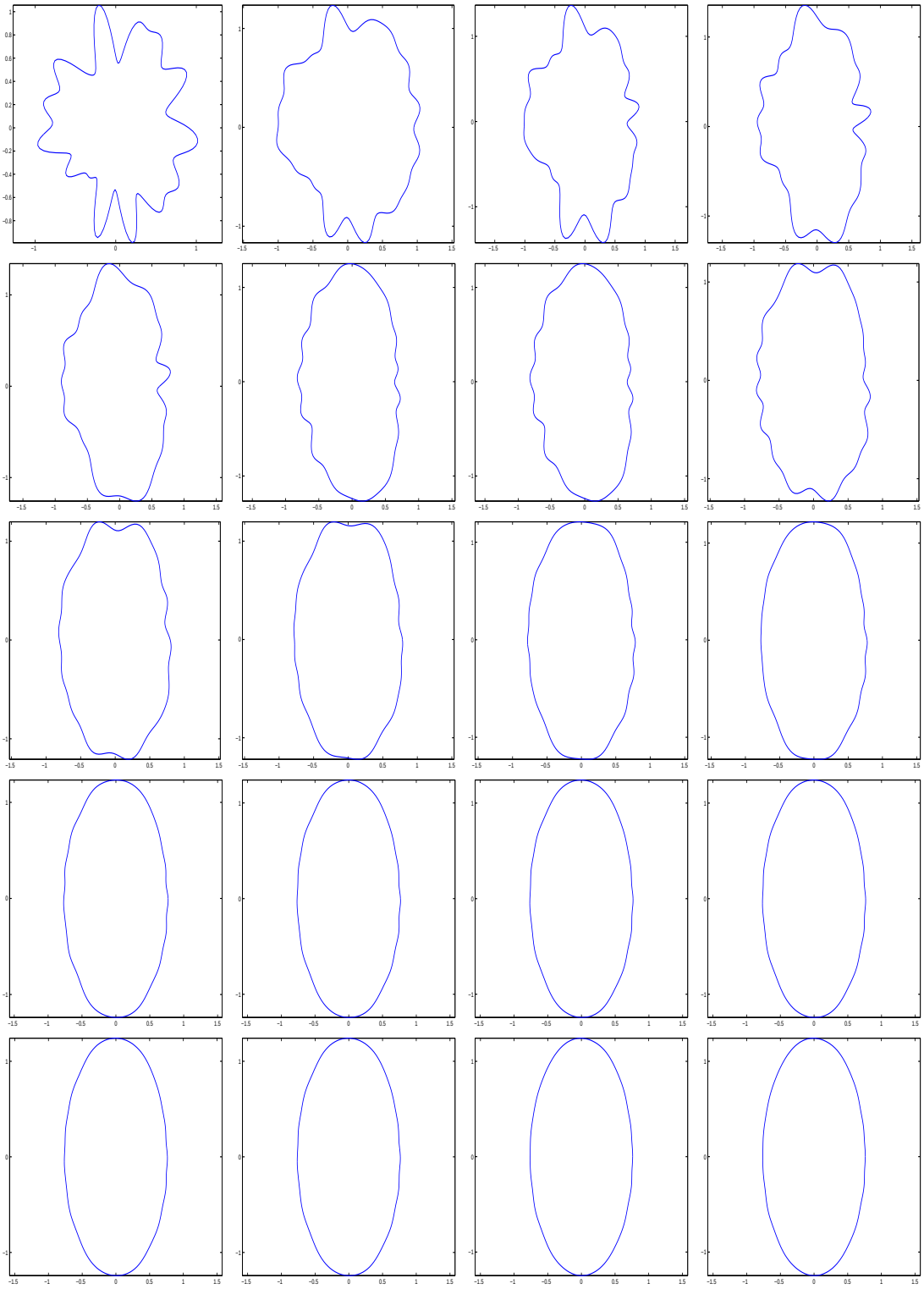

FIGURE 4.4. Resulting domains with respect to problem (P2) computed by the Quasi-Newton method for the penalty functional.

References

[1] N.V. Banichuk. Optimization of elastic bars in torsion. *International Journal of solids and Structures*, 12:275–286, 1976.

[2] N.V. Banichuk and B.L. Karihaloo. Minimum-weight design of multi-purpose cylindrical bars. *International Journal of solids and Structures*, 12:267–273, 1976.

[3] S. Belov and N. Fujii. Symmetry and sufficient condition of optimality in a domain optimization problem. *Control and Cybernetics*, 26:45–56, 1997.

[4] G. Beylkin, R. Coifman, and V. Rokhlin. The fast wavelet transform and numerical algorithms. *Comm. Pure and Appl. Math.*, 44:141–183, 1991.

[5] A. Cohen, I. Daubechies, and J.-C. Feauveau. Biorthogonal bases of compactly supported wavelets. *Pure Appl. Math.*, 45:485–560, 1992.

[6] W. Dahmen. Wavelet and multiscale methods for operator equations. *Acta Numerica*, 6:55–228, 1997.

[7] W. Dahmen, H. Harbrecht, and R. Schneider. Wavelets on manifolds II: Application to boundary element methods and pseudodifferential equations. in preperation.

[8] W. Dahmen and A. Kunoth. Multilevel preconditioning. *Numer. Math.*, 63:315–344, 1992.

[9] W. Dahmen, S. Prößdorf, and R. Schneider. Wavelet approximation methods for pseudodifferential equations ii: Matrix compression and fast solution. *Advances in Computational Mathematics*, 1:259–335, 1993.

[10] W. Dahmen, S. Prößdorf, and R. Schneider. Multiscale methods for pseudodifferential equations on smooth manifolds. In C.K. Chui, L. Montefusco, and L. Puccio, editors, *Proceedings of the International Conference on Wavelets: Theory, Algorithms, and Applications*, pages 385–424, 1994.

[11] J.E. Dennis and J.J. Moré. A Characterization of Superlinear Convergence and its Application to Quasi-Newton Methods. *Math. Comp.*, 28:549–560, 1974.

[12] J.E. Dennis and R.B. Schnabel. *Numerical Methods for Nonlinear Equations and Unconstrained Optimization Techniques*. Prentice-Hall, Englewood Cliffs, 1983.

[13] K. Eppler. Boundary integral representations of second derivatives in shape optimization. *Discussiones Mathematicae (Differential Inclusion Control and Optimization)*, 20:63–78, 2000.

[14] K. Eppler. Optimal shape design for elliptic equations via BIE-methods. *J. of Applied Mathematics and Computer Science*, 10:487–516, 2000.

[15] K. Eppler. Second derivatives and sufficient optimality conditions for shape functionals. *Control and Cybernetics*, 29:485–512, 2000.

[16] A.V. Fiacco and G.P. McCormick. *Nonlinear Programming: Sequential Unconstrained Minimization Techniques*. Wiley, New York, 1968.

[17] R. Fletcher. *Practical Methods for Optimization, volume 1,2*. Wiley, New York, 1980.

[18] L. Greengard and V. Rohklin. A fast algorithm for particle simulation. *J. Comput. Phys.*, 73:325–348, 1987.

[19] Ch. Grossmann and J. Terno. *Numerik der Optimierung*. Teubner, Stuttgart, 1993.

[20] W. Hackbusch and Z.P. Nowak. On the fast matrix multiplication in the boundary element method by panel clustering. *Numer. Math.*, 54:463–491, 1989.

[21] H. Harbrecht, F. Paiva, C. Pérez, and R. Schneider. Biorthogonal wavelet approximation for the coupling of FEM-BEM. *Preprint SFB 393/99-32, TU Chemnitz*, 1999. to appear in Numer. Math.

[22] H. Harbrecht, F. Paiva, C. Pérez, and R. Schneider. Wavelet preconditioning for the coupling of FEM-BEM. *Preprint SFB 393/00-07, TU Chemnitz*, 2000. submitted to Numerical Linear Algebra with Applications.

[23] H. Harbrecht and R. Schneider. Wavelet Galerkin Schemes for 2D-BEM. In *Operator Theory: Advances and Applications*, volume 121. Birkhäuser, (2001).

[24] J. Haslinger and P. Neitaanmäki. *Finite Element Approximation for Optimal Shape, Material and Topological Design, 2nd edition.* Wiley, Chichester, 1996.

[25] O. Pironneau. *Optimal Shape Design for Elliptic Systems.* Springer, New York, 1983.

[26] G. Polya. Torsional Rigidity, Principal Frequency Electrostatic Capacity, and Symmetrization. *Quarterly of Applied Mathematics*, 6:267–277, 1948.

[27] R.T. Rockafellar. Augmented Lagrange Multiplier Functions and Duality in Nonconvex Programming. *SIAM J. Control*, 12:268–285, 1974.

[28] R. Schneider. *Multiskalen- und Wavelet-Matrixkompression: Analysisbasierte Methoden zur Lösung großer vollbesetzter Gleichungssyteme.* B.G. Teubner, Stuttgart, 1998.

[29] J. Sokolowski and J.-P. Zolesio. *Introduction to Shape Optimization.* Springer, Berlin, 1992.